BIOCHEMICAL PHARMACOLOGY 75 (2008) 1083–1092

available at www.sciencedirect.com

ScienceDirect

journal homepage: www.elsevier.com/locate/biochempharm

Inhibition of glioblastoma growth and angiogenesis by gambogic acid: An *in vitro* and *in vivo* study

Lei Qiang [a,1], *Yong Yang* [a,1], *Qi-Dong You* [b,*], *Yan-Jun Ma* [a], *Lan Yang* [a], *Fei-Fei Nie* [a], *Hong-Yan Gu* [a], *Li Zhao* [a], *Na Lu* [a], *Qi Qi* [a], *Wei Liu* [a], *Xiao-Tang Wang* [c], *Qing-Long Guo* [a,**]

[a] *Department of Physiology, Jiangsu Key Laboratory of Carcinogenesis and intervention, China Pharmaceutical University, Nanjing 210009, People's Republic of China*

[b] *Department of Medicinal Chemistry, China Pharmaceutical University, Nanjing 210009, People's Republic of China*

[c] *Department of Chemistry and Biochemistry, Florida International University, Miami, FL 33199, USA*

ARTICLE INFO

Article history:
Received 26 July 2007
Accepted 28 October 2007

Keywords:
Gambogic acid
Apoptosis
Glioblastoma
Angiogenesis
Caspase
Mitochondrion

JEL classification:
Neuropharmacology

ABSTRACT

Gambogic acid (GA) is the major active ingredient of gamboge, a brownish to orange resin exuded from *Garcinia hanburryi* tree in Southeast Asia. The present study aims to demonstrate that gambogic acid (GA) has potent anticancer activity for glioblastoma by *in vitro* and *in vivo* study. Rat brain microvascular endothelial cells (rBMEC) were used as an in vitro model of the blood–brain barrier (BBB). To reveal an involvement of the intrinsic mitochondrial pathway of apoptosis, the mitochondrial membrane potential and the western blot evaluation of Bax, Bcl-2, Caspase-3, caspase-9 and cytochrome c released from mitochondria were performed. Angiogenesis was detected by CD31 immunochemical study. The results showed that the uptake of GA by rBMEC was time-dependent, which indicated that it could pass BBB and represent a possible new target in glioma therapy. GA could cause apoptosis of rat C6 glioma cells in vitro in a concentration-dependent manner by triggering the intrinsic mitochondrial pathway of apoptosis. *In vivo* study also revealed that i.v. injection of GA once a day for two weeks could significantly reduce tumor volumes by antiangiogenesis and apoptotic induction of glioma cells. Collectively, the current data indicated that GA may be of potential use in treatment of glioblastoma by apoptotic induction and antiangiogenic effects.

1. Introduction

Glioblastoma multiforme is the most common malignant central nervous system (CNS) tumor in adults. Glioma cells show a high proliferation rate and diffusely infiltrate adjacent brain tissues [1]. Invasive glioblastoma cells rapidly infiltrate and disrupt normal tissue architecture, making complete surgical removal virtually impossible. Despite aggressive therapeutic approaches combining surgical resection, radiotherapy, and chemotherapy, the mean survival time of patients diagnosed with glioblastoma is only ~1 year [2–4]. Consequently, development of novel drug for glioblastoma multiforme is very important.

* *Corresponding author*. Tel.: +86 25 83271055; fax: +86 25 83271055.
** *Corresponding author*. Tel.: +86 25 83271351; fax: +86 25 83271351.
E-mail addresses: youqidong@gmail.com (Q.-D. You), anticancer_drug@yahoo.com.cn (Q.-L. Guo).

[1] These authors contributed equally.

0006-2952/$ – see front matter
doi:10.1016/j.bcp.2007.10.033

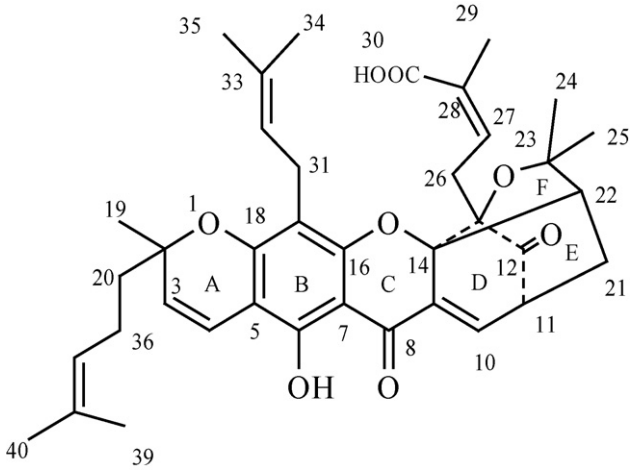

Fig. 1 – Chemical structure of GA.

Gambogic acid (GA, Fig. 1) is the major active ingredient of gamboge, a brownish to orange resin exuded from *Garcinia hanburryi* tree in Southeast Asia [5,6]. The structure of this natural product has been firmly established from both detailed NMR spectroscopic analysis [7] and X-ray crystallographic studies [8]. We have previously demonstrated that GA, used in traditional Chinese medicine, had potent anticancer activity for kinds of non-SNC carcinoma *in vitro* and *in vivo* [9–14]. This led us to question whether GA could exert similar effects in glioma cells as well as in animal glioma models.

The present study demonstrated that GA reduces cellular viability of rat C6 glioma cells and induced apoptosis of C6 cells. These findings were confirmed in vivo using a C6 orthotopic glioma rat model. The tumor volumes were reduced by up to 87% following i.v. administration of 2 mg/kg GA. In parallel, GA-treated animals exhibited improved clinical outcome and higher survival rate. In addition, in drug-treated animals, tumors exhibited an upregulation of the proapoptotic proteins Bax and cleaved caspase-3. Furthermore, reduced tumor microvessel density measured in vivo through CD 31 immunohistochemistry was observed.

2. Methods

2.1. Materials

GA was isolated from gamboge resin of *G. hanburyi*, with the purity of 99% as determined by HPLC according to previous study [15]. It was dissolved at a concentration of 0.01 mol/L in 100% DMSO as a stock solution, stored at −20 °C, and diluted with medium before each experiment. The final DMSO concentration did not exceed 0.1% DMSO throughout the study (in our study, all the control groups are composed of 0.1% DMSO). ^{125}I-labeled GA was offered by Wuxi Nuclear Medical Institute (Jiangsu, China). MTT (3-(4,5-dimethylthiazol-2-yl)-2,5-diphenyl tetrazolium bromide) was purchased from Fluka, USA and was dissolved in 0.01 M PBS. Primary antibodies were obtained from Santa Cruz Biotechnology Inc. (USA), and IRDye^{TM}800 conjugated anti-goat and anti-rabbit second antibodies were obtained from Rockland Inc. (USA). JC-1 probe was from Molecular Probes, Inc. (Eugene, OR).

2.2. Cell culture

Rat C6 glioma cell line was purchased from Cell Bank of Shanghai Institute of Biochemistry and Cell Biology, Shanghai Institutes for Biological Sciences, Chinese Academy of Sciences. The cells were cultured in DMEM, supplemented with 10% (v/v) fetal calf serum, 100 U/mL penicillin and 100 U/mL streptomycin in a 5% CO_2 atmosphere.

Rat brain microvascular endothelial cells (rBMEC) were isolated from the cerebral gray matter of rat brains [16]. The isolated cerebral gray matter was digested with trypsin (0.05%) at 37 °C for 20 min, then filtered through 149-μm nylon mesh, after which the filtrate was collected. The filtrate was filtered through 79-μm nylon mesh and the matter on the nylon mesh was collected. Then the matter was digested with type II collagenase (0.1%) at 37 °C for 20 min and centrifuged at room temperature for 5 min (200 × *g*), and the cells were collected. The isolated rBMEC were seeded in cultured flasks coated with gelatin (2%) and cultured at 37 °C in culture medium. The culture medium (pH 7.4) consisted of high glucose DMEM and F-12 medium (1:1) containing 20% fetal bovine serum, L-glutamine (0.9 g/L), heparin (50 mg/L), streptomycin (105 U/mL), penicillin (105 U/mL) and $NaHCO_3$ (0.5 g/L). On the 4th day after seeding, the culture medium was replaced, after which the culture medium was replaced every 2 days. On day 12, the rBMEC were transferred to 24-well plates coated with gelatin (2%) and cultured at 37 °C for 12–14 days. Transport experiments were performed when the cells reached confluence. Cultured rBMEC were identified by an immunostaining method using factor-VIII related antigen.

2.3. Transport experiment

When cells reached confluence after 12–14 days, uptake experiments were performed. Briefly, the cultured cell monolayer was washed three times with 1 mL of pH 7.4 Hanks' solution (isotonic buffer) containing NaCl (0.137 mol/L), KCl (5.37 mmol/L), $CaCl_2$ (1.26 mmol/L), $MgSO4{\cdot}7H_2O$ (0.81 mmol/L), $Na_2HPO4{\cdot}H_2O$ (0.37 mmol/L), KH_2PO4 (0.44 mmol/L), $NaHCO_3$ (4.17 mmol/L), and glucose (2.92 mmol/L) at 37 °C. The cultured cells were pre-incubated at 37 °C for 30 min in Hanks' solution. After the pre-incubation, the solution was removed, and Hanks' solution (0.3 mL) containing ^{125}I-labeled GA was added to each well, then the final concentration was 0.3 μM (1 μCi/mL). To terminate the transport reaction, cells were washed three times with 0.5 mL ice-cold Hanks' solution at the designated time. 5, 10, 15, 30, 60 min later and were rapidly washed three times with ice-cold NaCl (0.9%). Then cells were harvested and then frozen thawed three times followed by immediate centrifugation (10,000 × *g* for 10 min at 4 °C). Radioactivity and protein contents of the supernatant were determined by the automatic gamma counter and Bradford methods, respectively.

2.4. Cell growth inhibition assay

Rat C6 glioma cells were cultured in DMEM media as described above till mid-log phase. Different concentrations of GA were

added and incubated for 24 h. At the end of incubation, the morphology of cells was monitored under an inverted light microscope. The culture medium was removed and 20 μl of 5 mg/ml MTT was added. Four hours later, the supernatant was discarded and 100 μl of DMSO was added to each well. The mixture was shaken and measured at 570 nm using a Universal Microplate Reader (EL800, BIO-TEK INSTRUMENTS INC). Cell Inhibition ratio (*I*%) was calculated by the following equation:

$$I\% = \left(\frac{A_{\text{control}} - A_{\text{treated}}}{A_{\text{control}}}\right) \times 100$$

where A_{treated} and A_{control} are the average absorbance of three parallel experiments from treated and control groups, respectively. The IC_{50} was taken as the concentration that caused 50% inhibition of cell proliferation and was calculated by SAS statistical software.

2.5. Cell morphological assessment

Rat C6 glioma cells were cultured in DMEM till mid-log phase. Three doses of GA (1, 1.5, 2 μM) were then added to the culture media and incubated for an additional 24 h. At the end of incubation, the morphology of cells was monitored under an inverted light microscope. All floating and attached cells were harvested with 0.02% (w/v) EDTA and 0.25% (w/v) trypsinase. The cell suspension was fixed with ice-cold 4% paraform for 20 min and washed with ice-cold PBS. Then cell suspension was permeabilized with 0.3% triton x-100, washed with ice-cold PBS, stained with fluorochrome dye DAPI (Santa Cruz, USA) and observed under a fluorescence microscopy (OlympusIX51, Japan) with a peak excitation wavelength of 340 nm.

Rat C6 glioma cells were treated with GA (1, 1.5, 2 μM) for 24 h. The cells were collected and fixed with 3% glutaraldehyde and washed with PBS 0.1 mol/L. Then the cells were fixed with 1% osmic acid and dehydrated by ethanol in gradient concentration. Embedded with EPOr812 and divided to ultraslice, cells were double-stained with uranium acetate and plumbum citrate. The changes were observed with transmission electron microscopy.

2.6. Measurement of mitochondrial membrane potential (Ψ_m)

Changes in Ψ_m were monitored by the uptake of JC-1. Rat C6 glioma cells were cultured in DMEM till mid-log phase. Three doses of GA (1, 2.5, 5 μM) were then added to the culture media and the cells were continuously incubated for an additional 2 h. The process of labeling with JC-1 was performed according to the mitochondrial membrane potential assay kit manual. Then, the samples labeled with JC-1 were analysed with flow cytometer (FACSCalibur, Becton Dickinson, USA) with settings of FL1 at 530 nm and FL2 at 585 nm. JC-1 is a lipophilic cationic dye which accumulates and forms aggregates in normal mitochondria with a high negative membrane potential, in which condition it emits a red–orange fluorescence, detected at 585 nm, whereas in mitochondria with low membrane potential it forms monomers in the cytosol that emit a green fluorescence, detected at 530 nm [17].

2.7. Animals

Spraque–Dawley rats (Charles River Laboratories, Sulzfeld, Germany) weighting 200–250 g were used. Animals were housed in groups of two under standard conditions at a temperature of 22 °C ± 1 and a 12-h light–dark cycle with free access to food and water. All experiments were carried out according to the National Institutes of Health Guide for the Care and Use of Laboratory Animals (publication no. 85-23, revised 1985) and approved by IACUC (Institutional Animal Care and Use Committee of China Pharmaceutical University).

2.8. Orthotopic glioma model

Before implantation, 85–90% confluent C6 cells were trypsinized, rinsed with DMEM + 10% fetal calf serum, and centrifuged at 1000 rpm for 4 min. The cell pellet was resuspended in DMEM and placed on ice. Concentration of viable cells was adjusted to 1×10^5 cells/1 μl of DMEM. Each rat was anesthetized and placed in a stereotactic frame, and a hole was drilled at AP 0.0, R –3.0 relative to bregma according to the stereotaxic atlas of König and Klippel [18]. Tumor cells were injected at a rate of 0.5 μl/s, using a 2 μl Hamilton (#2701) syringe (Reno, NV, USA) with a 26s-gauge needle mounted on a stereotactic holder at a depth of 5 mm. The needle was left in place for a further 10 min to prevent reflux along the needle tract [19,20]. Then rats were divided into five groups. The negative control group was administrated with vehicle. The positive control was i.v. injected with 10 mg/kg Carmustine. The other three groups were treated with GA (0.5, 1, 2 mg/kg) intravenously 24 h after surgery, respectively. All drugs were given once a day and continued for two weeks.

Four micrometer-thick sections from formalin-fixed and paraffin-embedded tissues were placed on poly-L-lysine-coated slides for immunohistochemistry study. Sections for hematoxylin-eosin (HE)-staining were placed onto uncoated slides. Sections immunohistochemically processed for CD31 assays were placed onto coated slides. Images of HE-stained sections containing tumors were captured with a charge-coupled device camera by bright-field microscopy. The maximum cross-sectional area of the intracranial glioblastoma xenografts was determined by computer-assisted image analysis using a Leica Quantimet 500-system (Leica, Hamburg, Germany). The tumor volume was estimated using the formula: volume = (square root of maximal tumor cross-sectional area)^3 [21].

2.9. Western-blot analysis for Bcl-2, Bax, pro-caspase-3,pro-caspase-9 and cytochrome c proteins

C6 cells were cultured in DMEM till mid-log phase and then incubated with 1×10^{-6}, 1.5×10^{-6} and 2×10^{-6} M GA for 24 h. Proteins were isolated by lysis buffer (100 mM Tris–Cl, pH 6.8, 4% (m/v) SDS, 20% (v/v) glycerol, 200 mM β-mercaptoethanol, 1 mM PMSF, and 1 g/ml aprotinin) and measured using the BCA protein assay method with Varioskan spectrofluorometer and spectrophotometer (Thermo) at 562 nm. The fractionation of the mitochondrial protein and cytosolic protein was performed according to the mitochondria/cytosol fractionation kit (Biovision Research Products) instruction. Protein

samples were separated with 15% SDS-polyacrylamide gel (SDS-PAGE) and transferred onto the PVDF membranes (Millipore). Immune complexes were formed by incubation of the proteins with primary antibodies, mouse anti-Bax (Santa Cruz Biotechnology), rabbit anti-Bcl-2 (Santa Cruz Biotechnology), rabbit anti-caspase-3 (Santa Cruz Biotechnology), rabbit anti-caspase-9 (Santa Cruz Biotechnology), mouse anti-cytochrome c (Biosouce international), mouse anti Cox IV (Abcam) and mouse anti-Actin (Boster Inc, China) overnight at 4 °C. Blots were washed and incubated for 1 h with IRDye™800 conjugated anti-goat and anti-rabbit second antibodies. All antibodies were obtained from Santa Cruz Biotechnology, CA, USA. Immunoreactive protein bands were detected with an Odyssey Scanning System (LI-COR inc., USA).

2.10. Immunohistochemistry and microvessel counts

The expression of PECAM-1/CD-31 was assessed by SP immunohistochemical method using a mouse-anti-rat CD-31 monoclonal antibody clone TLD-3A12 (SEROTEC) and an UltraSensitive™ S-P kit (kit 9710 MAIXIN). The deparaffinized sections were boiled in citrate buffer at high temperature and high pressure for antigen retrieval, and then incubated with the antibody at 4 °C overnight. Immunohistochemical staining was then performed according to the UltraSensitiveTM S-P kit manual. Counter staining was done with Harris hematoxylin. All reagents were supplied by Maixin-Bio Co, Fuzhou, China. Microvessel counts (MVCs) were assessed according to Weidner [22]. The hot spots were selected under a microscope (100×), then individual counts were made under 400× field (NIKON YS100 microscope, 0.155 mm^2 per field). The average counts in five fields were recorded. Any single highlighted endothelial cell or endothelial cell cluster clearly separated from adjacent microvessels, and distinct clusters of brown-staining endothelial cells were counted as separate microvessels. Vessel lumens were not the sole criteria in identifying a microvessel.

2.11. Statistical evaluation

All results shown represent the Mean ± S.E.M. from triplicate experiments performed in a parallel manner unless otherwise indicated. Statistical analyses were performed using an unpaired, two-tailed Student's *t*-test. All comparisons are made relative to untreated controls and significance of difference is indicated as $^*P < 0.05$.

3. Results

3.1. Uptake of GA by rBMEC

To determine if GA could enter blood–brain barrier (BBB), the GA uptake activity of primary cultured rBMEC cells was measured. After rBMEC cells were incubated with a medium containing 0.3 μM ^{125}I-labeled GA (1 μCi/mL) at 37 °C for a total time of 60 min, the amounts of ^{125}I-labeled GA taken up by cells were measured at 5, 10, 15, 30, and 60 min. The results indicated that the uptake of GA by rBMEC was time-dependent (Fig. 2A). So GA might be able to enter BBB, which was consisted with our previous report that GA could distribute in the central nervous system [23].

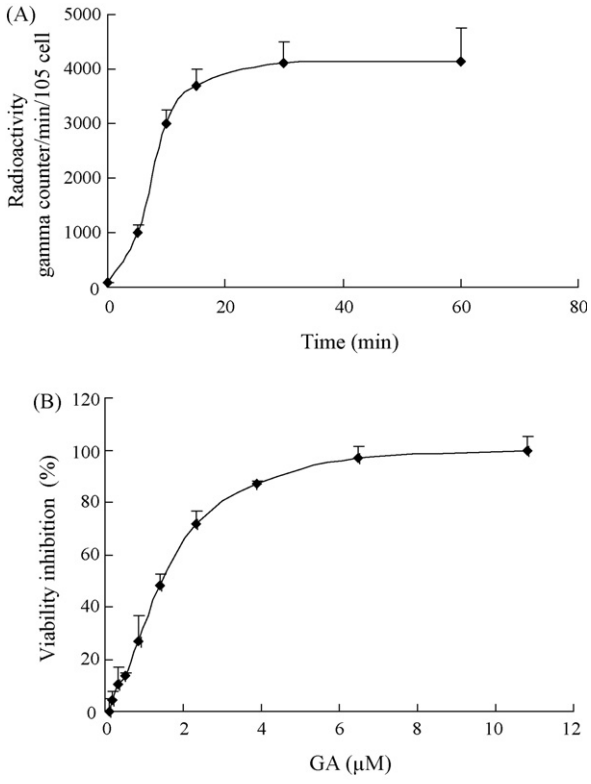

Fig. 2 – (A) Uptake of GA by rBMEC over time. Cells were incubated with a medium containing 0.3 μM ^{125}I-labled GA at 37 °C for 60 min. (B) GA reduced cellular viability of rat glioma cells *in vitro*. Viability of rat C6 glioma cells incubated with GA was assessed using the MTT-assay. Data are presented as the mean ± S.E.M., determined from six separate experiments.

3.2. Reduced cellular viability of rat C6 glioma cells

Viability of rat C6 glioma cells was assessed after incubation with increasing concentrations of GA for 24 h. The results indicated that GA significantly reduced the cellular viability of C6 rat glioma cells in a concentration-dependent manner (Fig. 2B). The IC_{50} value was 1.2 μmol/L.

3.3. Induction of apoptotic cell death in vitro

After treatment with GA, C6 glioma cells were severely distorted, grew slowly and some cells turned round in shape. The untreated cells displayed normal, healthy shapes demonstrated by the clear skeletons (Fig. 3A). To assess whether GA could induce apoptotic cell death in vitro, cells were stained with fluorochrome dye DAPI and the nucleolus changes were observed under a fluorescence microscopy. Untreated cells were stained equally blue fluorescence which showed that chromatins of untreated cells were equably distributed in nucleolus. After GA treatment, chromatins congregated and emitted bright fluorescence as well as nucleolus pyknosis, the

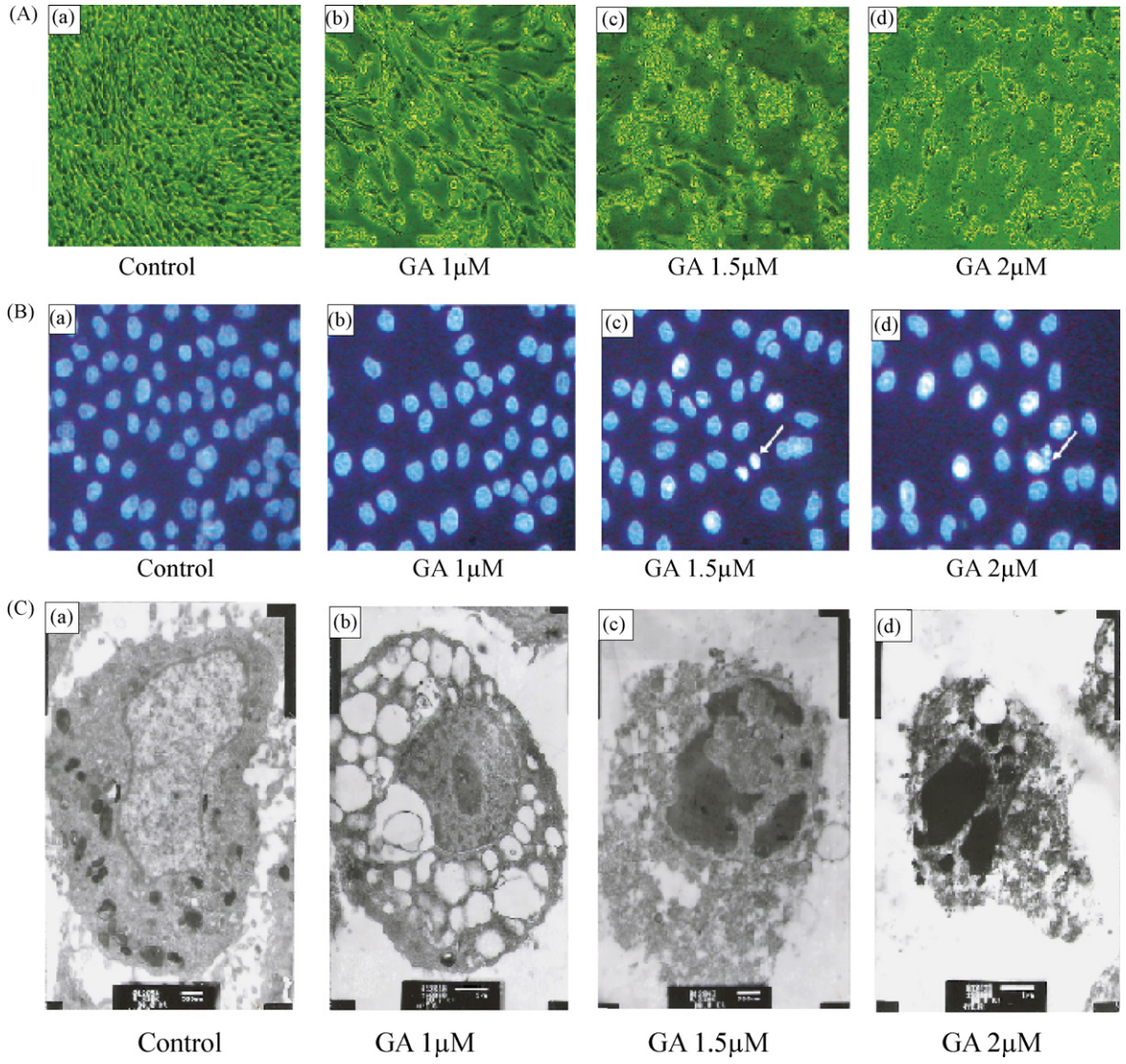

Fig. 3 – GA induced C6 glioma cells apoptosis. (A) Morphologic change of cells observed under an inverted light microscope (×400). (B) DAPI staining; the arrow indicates a typical apoptotic cell. (C) Characteristic morphology of GA-induced apoptosis of C6 glioma cells under electron microscope (×6000).

early phenomena of apoptosis (Fig. 3B). To further confirm the results, transmission electron microscopy was used to observe the apoptotic morphology. Under electron microscope, the reduced cell volume and shrunk cytoplasm could be observed in GA-treated cells. But plasma membrane remained well defined and condensed chromatins located along nuclear envelope or formed irregularly shaped crescents at nuclear edges (Fig. 3C).

GA-induced apoptosis was associated with mitochondrial depolarization in C6 glioma cells proved by a potentiometric probe, the carbocyanine JC-1. Green-positive, red-negative events (LR-quadrant) were scored as depolarized cells. The results indicated that the control group showed 4% cell of green fluorescence, while increasing to 21%, 45% and 87% after 1, 2.5 and 5 μM GA treated for 2 h, respectively (Fig. 4A).

To further confirm the results, the levels of Bcl-2, Bax, Pro-caspase-3, Pro-caspase-9, cytosolic cyt-c and mitochondrial cyt-c-expression were evaluated. Densitometric analysis showed the protein levels of either Bax or cytosolic cyt-c were upregulated in response to GA treatment, followed by a significant decrease in Bcl-2, Pro-caspase-3, Pro-caspase-9 and mitochondrial cyt-c protein level (Fig. 4B).

3.4. *Significantly reduced tumor volume and induced apoptotic cell death in the rat glioma model*

In order to confirm the antineoplastic effects of GA for glioblastoma *in vivo*, C6 glioma cells were injected in rat striatum and treated with 0.5, 1, 2 mg/kg GA or vehicle for two weeks ($n = 5$ per group) starting 24 h after initial tumor cell injection. The GA-treated animals showed a dramatic reduction of tumor volume at 14 days of treatment (Fig. 5A, b; c; d) compared with vehicle-treated animals (Fig. 5A, a). Moreover, the HE staining results revealed that the glioma model rat treated with GA exhibited better defined tumor margins and fewer invasive cells to the contralateral striatum compared

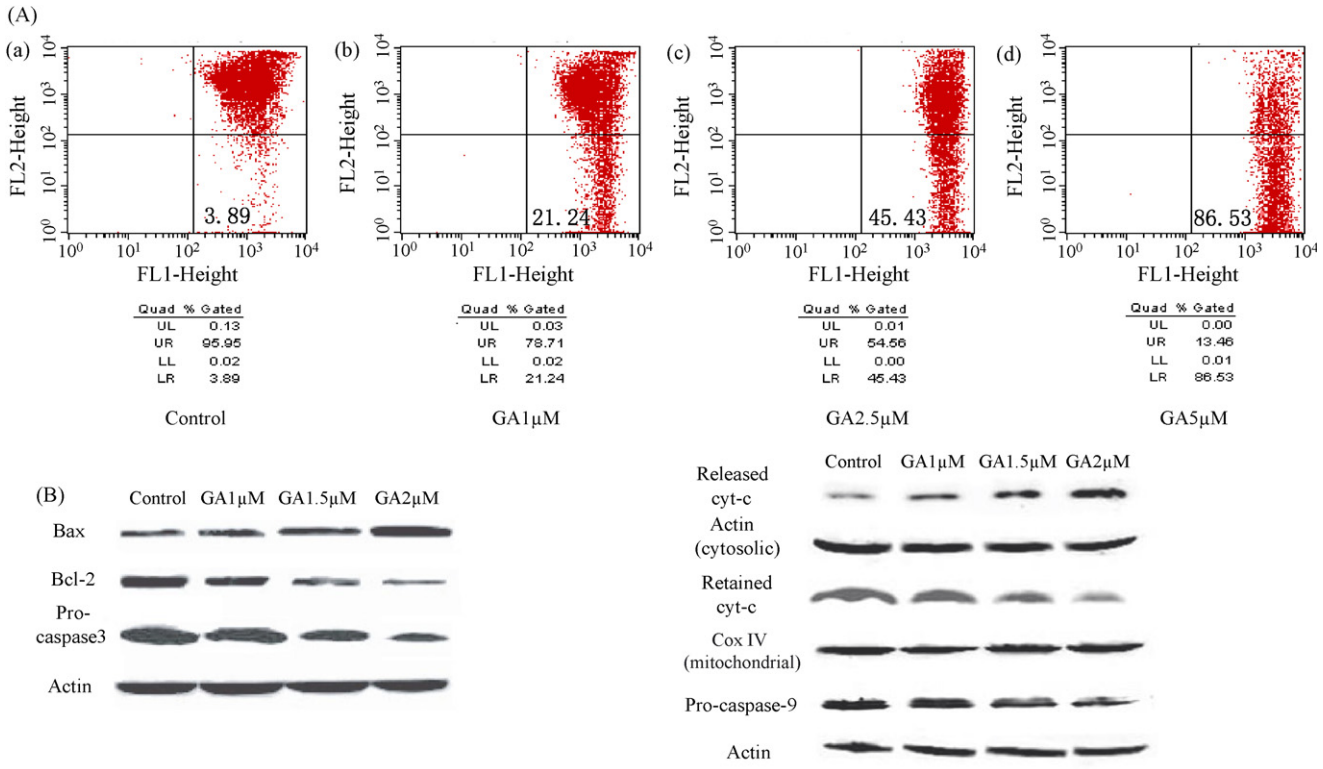

Fig. 4 – GA induced C6 glioma cells apoptosis maybe through the intrinsic mitochondrial pathway. (A) The percentage of events associated with positive-green and negative-red fluorescence (LR-quadrant) was scored as mitochondrial-depolarized cells. (B) Bcl-2, Bax, pro-caspase-3, pro-caspase-9, cytosolic cyt-c and mitochondrial cyt-c expressions in cultured C6 glioma cells treated by 1, 1.5 and 2 μM GA, respectively. (For interpretation of the references to color in this figure legend, the reader is referred to the web version of the article.)

with the vehicle control and carmustine treated rats. Vehicle treated animals exhibited a median tumor volume of 350.2 $mm^3 \pm 70.0$, whereas 0.5, 1, 2 mg/kg GA-treated animals revealed tumor volumes of 280.4 $mm^3 \pm 55.5$, 96.8 $mm^3 \pm 25.0$, 47.2 $mm^3 \pm 32.0$, reflecting 20%, 72% and 87% reduction, respectively. Carmustine treatment reduced tumor volumes by 44% after 14 days (Fig. 5C). At day 14, rats in GA-treated groups exhibited improved clinical outcome and higher surviving rate compared with the vehicle treated group (Fig. 6A).

To assess if GA induces apoptotic cell death in vivo, the expressions of antiapoptotic protein Bcl-2, the proapoptotic proteins Bax and Pro-caspase-3 were detected in whole-hemisphere lysates of C6 glioma animals and controls. Densitometric analysis at the endpoint of treatment revealed that protein levels of either Bax or Pro-caspase-3 were upregulated and Bcl-2 was decreased in GA-treated groups (Fig. 6B).

3.5. *MVCs in vivo*

Intratumoral vessel densities were quantified after staining histological sections for CD 31, which specifically labels endothelial cells. In 0.5, 1 and 2 mg/kg GA-treated rats, the mean intratumoral microvessel densities, as counted in three randomly selected hpfs, were reduced by 30%, 65% and 82% relative to tumors in the control group ($P < 0.05$ vs. Control; Fig. 5D). While MVCs of carmustine treated rats had significant changes compared with the control. The vasculature in the surrounding normal brain tissues was not affected by the treatment.

4. Discussion

Rat brain microvascular endothelial cells (rBMEC) were used as an in vitro model of the blood–brain barrier [16]. In this study, rBMEC could uptake GA in a time-dependent manner, which was consisted with the previous pharmacokinetics study of GA in rats and represented a possible new candidate drug for glioma therapy [23].

The current data demonstrated antineoplastic potency of GA *in vitro* by inhibition of cellular growth and induction of cell apoptosis of rat C6 glioma cells. According to the results, the expression of Bcl-2 was decreased, while Bax as well as its downstream target cleaved caspase-3 peaked after treatment with GA. The ratio of Bcl-2 and Bax was reduced significantly. Bcl-2 and Bax are two kinds of apoptosis related proteins [24,25], and caspase-3 is in the downstream of Bcl-2 and Bax. They all play important roles in the control of apoptosis initiation and execution. Recent researches showed that Bax could form heterodimers with Bcl-2 to inhibit the anti-apoptotic function of Bcl-2. Hence Bcl-2/Bax ratio is important to apoptosis induced by several agents and the decline of this

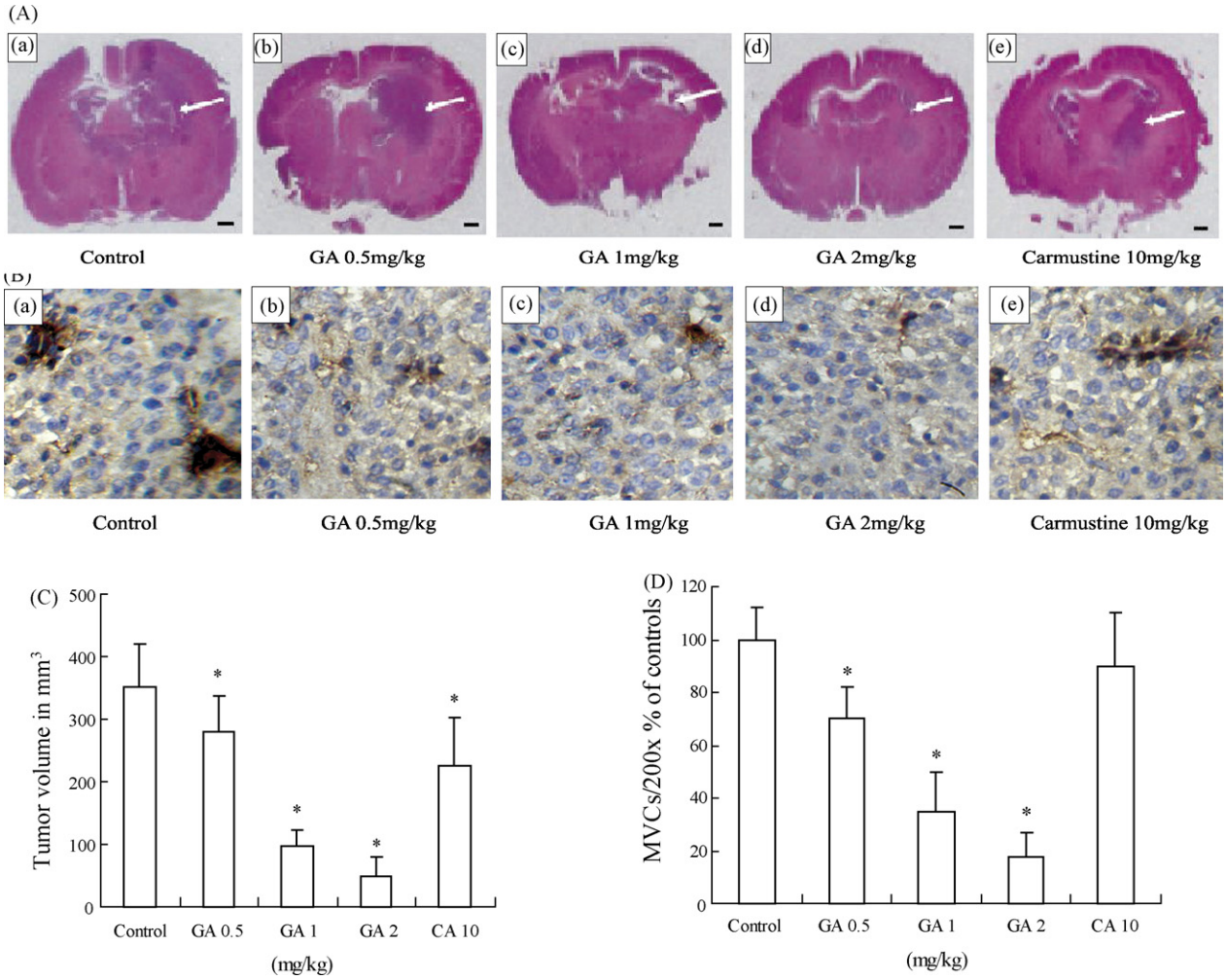

Fig. 5 – Administration of GA significantly reduced tumor growth and angiogenesis in the rat glioma model. (A) A magnification of the striatum with a representative part of the tumor by HE staining. GA-treated animals showed significantly smaller tumor volumes (b, c, d) compared to untreated animals (a). Bar: 1 mm. (B) Immunostaining for CD 31 revealed numerous small capillaries in transplanted tumors. GA-treated animals showed significantly less CD 31 positive small capillaries (b, c, d) compared to untreated animals. (C) Tumor volumes in mm^3 of GA-treated animals compared with vehicle-treated animals. (D) Vessel densities in three randomly selected fields were reduced significantly in tumors from GA-treated animals. Control: vehicle treated animals; GA: GA-treated animals. CA: Carmustine served as a positive control. Data are presented as mean ± S.E.M. of five animals per group. Asterisks indicate significant level in Student *t*-test: (*) $p < 0.05$ ($n = 5$).

ratio contributes to apoptosis induction. In addition, Bax dimers or oligomers directly form channel in mitochondrial outer membrane in apoptosis [25]. As mitochondrion plays a central role in the regulation of apoptosis of cancer cells [26,27], in this study, we also found that GA treatment for 2 h could significantly caused mitochondria depolarization and Ψ_m collapse, which could enhance cytochrome C and apoptosis inducing factor (AIF) releasing from mitochondrion [28]. So mitochondria might be one of the targets of GA. Our recent research reveals that GA can distribute into the intracellular cancer cells and inhibit mitochondrial complex I (data not shown). Although recent study revealed an undiscovered link between transferrin receptor (TfR) and the rapid activation of apoptosis and GA binding to TfR induced a unique signal leading to rapid apoptosis of tumor cells [29], we suggested that perhaps the extrinsic and intrinsic apoptotic pathways were both involved in the signal transduction of GA.

To verify these results *in vivo*, C6 cells were injected into rat striatum and continuously treated with GA i.v. for two weeks. GA treatment reduced tumor volume by up to 87%. Furthermore, preservation of neurological function and higher surviving rate were observed in GA-treated animals. At the endpoint of GA therapy, an increase in cleaved caspase-3 and Bax and decrease of Bcl-2 were observed. These findings indicated that GA induced apoptosis of rat C6 gliomas and contributed at least in part to the observed reduction in tumor volume.

Glioblastomas not only grow as solid tumor foci but also spread diffusely throughout the brain by high formation of

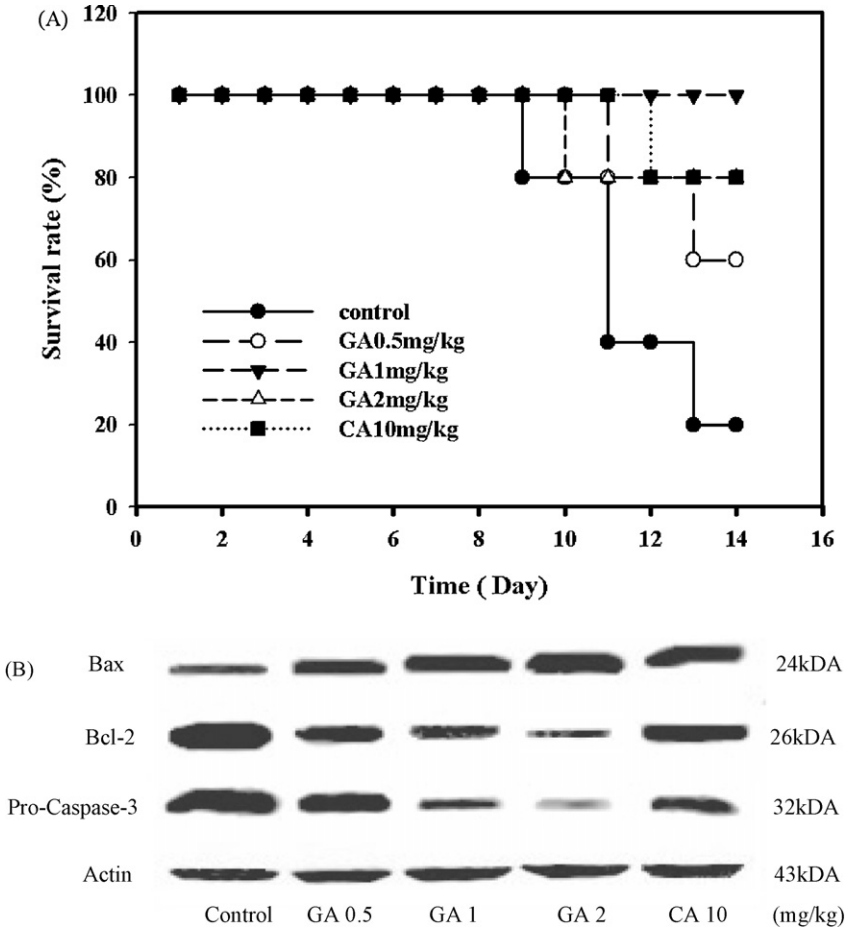

Fig. 6 – GA treatment improved the survival rate of animals and induced Bax, Bcl-2 and pro-caspase-3 expression *in vivo*. (A) The survival rate of the animals. (B) Bcl-2, Bax and pro-caspase-3 expressions in whole-hemisphere lysates of C6 rat glioma animals and control after 14 days of GA treatment. Control: vehicle treated animals; GA: GA-treated animals. CA: Carmustine served as a positive control.

new blood vessels. Therefore, antiangiogenic therapies are considered promising [30–33]. In the study, HE staining revealed that the glioma model rat treated with GA exhibited better defined tumor margins and fewer invasive cells to the contralateral striatum compared with the vehicle control and carmustine treated rats, which led us to further investigate the effect of GA on angiogenesis. Our previous study also provided evidences that GA had a potent antiangiogenic activity *in vitro*. It directly reduced vascular endothelial growth factor (VEGF)-stimulated human umbilical vein endothelial cells (HUVEC) proliferation, mobility and tube formation on matrigel. It also inhibited microvessel sprouting from vascular tissues and suppressed new vessel growth of chicken chorioallantoic membrane. To confirm the antiangiogenesis of GA *in vivo*, MVCs was conducted. The results showed significant decrease of MVCs in GA-treated rats. Although the exact mechanism of antiangiogenesis for GA remains unclear, our current research suggests that GA not only inhibits VEGF secreting of tumor cells, but also inhibits VEGF-mediated biological effects by inhibiting VEGF-induced tyrosine phosphorylation of KDR/Flk-1 and interfering with VEGF signal transduction, such as a significant decrease in VEGF-triggered p-ERK, p-AKT and p-p38 activation (data not shown).

However, the brain itself has a dense vascular bed, and gliomas preferentially invade along these vessels, a process that was recently termed ''vessel cooption'' [34]. Some reports also showed that inhibition of angiogenesis in an orthotopic glioblastoma model could strongly inhibit growth of the main tumor mass, but, in turn, favored glioma cell invasion along preexistent host vessels [35,36]. Therefore, therapeutic strategies that synchronously inhibit tumor angiogenesis, as well as tumor cell migration and proliferation appear to hold a greater promise than a mere antiangiogenic approach [21,37]. The dual anti-tumor and anti-angiogenetic activities of GA strongly indicate that it might create a potential new approach for glioma therapy. Such agents seem more promising in clinical practice than the compounds solely targeting angiogenesis (e.g., SU5416 and endostatin) [38–40].

Although the molecular basis of antineoplastic mechanisms of GA is yet not fully understood, it may offer a new therapeutic approach in human glioma therapy due to their positive effects on tumor cell apoptosis and negative effects of angiogenesis. GA would be readily available for glioma therapy in clinical studies. Further studies will be required to ascertain the optimal mode and timing for application of GA.

Acknowledgements

This work was supported by the National Natural Science Foundation of China (Nos. 30472044, 30701032 and 90713038) and Natural Science Foundation of Jiangsu province (No. BK20055096).

REFERENCES

[1] Kleihues P, Louis DN, Scheithauer BW, Rorke LB, Reifenberger G, Burger PC, et al. The WHO classification of tumors of the nervous system. J Neuropathol Exp Neurol 2002;61:215–25. discussion 26-9.
[2] Astner ST, Pihusch R, Nieder C, Rachinger W, Lohner H, Tonn JC, et al. Extensive local and systemic therapy in extraneural metastasized glioblastoma multiforme. Anticancer Res 2006;26:4917–20.
[3] Nieder C, Grosu AL, Astner S, Molls M. Treatment of unresectable glioblastoma multiforme. Anticancer Res 2005;25:4605–10.
[4] Stupp R, Mason WP, van den Bent MJ, Weller M, Fisher B, Taphoorn MJ, et al. Radiotherapy plus concomitant and adjuvant temozolomide for glioblastoma. N Engl J Med 2005;352:987–96.
[5] Auterhoff H, Frauendorf H, Liesenklas W, Schwandt C. The chief constituents of gamboge resins. 1. Chemistry of gamboges. Archiv der Pharmazie 1962;295(67):833–46.
[6] Liesenklas W, Auterhoff H. The constitution of gambogic acid and its isomerization. 4. Chemistry of gum-resin. Arch Pharm Berichte Dtsch Pharmazeutischen Ges 1966;299:797–8.
[7] Ollis WD, Ramsay MVJ, Sutherland IO, Mongkolsuk S. Constitution of gambogic acid. Tetrahedron 1965;21: 1453–70.
[8] Weakley TJR, Cai SX, Zhang H-Z, Keana JFW. Crystal structure of the pyridine salt of gambogic acid. J Chem Crystallogr 2002;31:501–5.
[9] Yu J, Guo QL, You QD, Lin SS, Li Z, Gu HY, et al. Repression of telomerase reverse transcriptase mRNA and hTERT promoter by gambogic acid in human gastric carcinoma cells. Cancer Chemother Pharmacol 2006;58:434–43.
[10] Wu ZQ, Guo QL, You QD, Zhao L, Gu HY. Gambogic acid inhibits proliferation of human lung carcinoma SPC-A1 cells in vivo and in vitro and represses telomerase activity and telomerase reverse transcriptase mRNA expression in the cells. Biol Pharm Bull 2004;27:1769–74.
[11] Zhao L, Guo QL, You QD, Wu ZQ, Gu HY. Gambogic acid induces apoptosis and regulates expressions of Bax and Bcl-2 protein in human gastric carcinoma MGC-803 cells. Biol Pharm Bull 2004;27:998–1003.
[12] Liu W, Guo QL, You QD, Zhao L, Gu HY, Yuan ST. Anticancer effect and apoptosis induction of gambogic acid in human gastric cancer line BGC-823. World J Gastroenterol 2005;11:3655–9.
[13] Guo QL, Lin SS, You QD, Gu HY, Yu J, Zhao L, et al. Inhibition of human telomerase reverse transcriptase gene expression by gambogic acid in human hepatoma SMMC-7721 cells. Life Sci 2006;78:1238–45.
[14] Jun Y, Guo QL, You QD, Zhao L, Gu HY, Yang Y, et al. Gambogic acid induced G2/M phase cell cycle arrest via disturbing CDK7 mediated phosphorylation of CDC2/P34 in human gastric carcinoma BGC-823 cells. Carcinogenesis 2006.
[15] IOSaSM WDOM. Tetrahron 1965;21:1453–70.
[16] Sun JJ, Xie L, Liu XD. Transport of carbamazepine and drug interactions at blood–brain barrier. Acta Pharmacol Sin 2006;27:249–53.
[17] Cossarizza A, Baccarani-Contri M, Kalashnikova G, Franceschi C. A new method for the cytofluorimetric analysis of mitochondrial membrane potential using the J-aggregate forming lipophilic cation 5,5′,6,6′-tetrachloro-1,1′,3,3′-tetraethylbenzimidazolcarbocyanine iodide (JC-1). Biochem Biophys Res Commun 1993;197: 40–5.
[18] KJaK RA. The rat brain: a stereotaxic atlas of the forebrain and lower parts of the brainstem. USA: Williams and Wilkins, Baltimore; 1963.
[19] Grommes C, Landreth GE, Sastre M, Beck M, Feinstein DL, Jacobs AH, et al. Inhibition of in vivo glioma growth and invasion by peroxisome proliferator-activated receptor gamma agonist treatment. Mol Pharmacol 2006;70:1524–33.
[20] Stander M, Naumann U, Dumitrescu L, Heneka M, Loschmann P, Gulbins E, et al. Decorin gene transfer-mediated suppression of TGF-beta synthesis abrogates experimental malignant glioma growth in vivo. Gene Ther 1998;5:1187–94.
[21] Brockmann MA, Papadimitriou A, Brandt M, Fillbrandt R, Westphal M, Lamszus K. Inhibition of intracerebral glioblastoma growth by local treatment with the scatter factor/hepatocyte growth factor-antagonist NK4. Clin Cancer Res 2003;9:4578–85.
[22] Weidner N. Current pathologic methods for measuring intratumoral microvessel density within breast carcinoma and other solid tumors. Breast Cancer Res Treat 1995;36:169–80.
[23] Guang-Ji HKLX-QW. Pharmacokinetics of gambogic acid in rats. J China Pharmaceut Univ 2005;4:338–41.
[24] Boise LH, Gonzalez-Garcia M, Postema CE, Ding L, Lindsten T, Turka LA, et al. bcl-x, a bcl-2-related gene that functions as a dominant regulator of apoptotic cell death. Cell 1993;74:597–608.
[25] Yin C, Knudson CM, Korsmeyer SJ, Van Dyke T. Bax suppresses tumorigenesis and stimulates apoptosis in vivo. Nature 1997;385:637–40.
[26] Green DR, Reed JC. Mitochondria and apoptosis. Science 1998;281:1309–12.
[27] Ceruti S, Mazzola A, Abbracchio MP. Resistance of human astrocytoma cells to apoptosis induced by mitochondria-damaging agents: possible implications for anticancer therapy. J Pharmacol Exp Ther 2005;314:825–37.
[28] He J, Xiao Y, Casiano CA, Zhang L. Role of mitochondrial cytochrome c in cocaine-induced apoptosis in coronary artery endothelial cells. J Pharmacol Exp Ther 2000;295: 896–903.
[29] Kasibhatla S, Jessen KA, Maliartchouk S, Wang JY, English NM, Drewe J, et al. A role for transferrin receptor in triggering apoptosis when targeted with gambogic acid. Proc Natl Acad Sci USA 2005;102:12095–100.
[30] Folkerth RD. Histologic measures of angiogenesis in human primary brain tumors. Cancer Treat Res 2004;117:79–95.
[31] Kargiotis O, Rao JS, Kyritsis AP. Mechanisms of angiogenesis in gliomas. J Neurooncol 2006;78:281–93.
[32] Sharma S, Sharma MC, Gupta DK, Sarkar C. Angiogenic patterns and their quantitation in high grade astrocytic tumors. J Neurooncol 2006;79:19–30.
[33] Naumov GN, Bender E, Zurakowski D, Kang SY, Sampson D, Flynn E, et al. A model of human tumor dormancy: an angiogenic switch from the nonangiogenic phenotype. J Natl Cancer Inst 2006;98:316–25.
[34] Holash J, Maisonpierre PC, Compton D, Boland P, Alexander CR, Zagzag D, et al. Vessel cooption, regression, and growth in tumors mediated by angiopoietins and VEGF. Science 1999;284:1994–8.

[35] Kunkel P, Ulbricht U, Bohlen P, Brockmann MA, Fillbrandt R, Stavrou D, et al. Inhibition of glioma angiogenesis and growth in vivo by systemic treatment with a monoclonal antibody against vascular endothelial growth factor receptor-2. Cancer Res 2001;61: 6624–8.
[36] Rubenstein JL, Kim J, Ozawa T, Zhang M, Westphal M, Deen DF, et al. Anti-VEGF antibody treatment of glioblastoma prolongs survival but results in increased vascular cooption. Neoplasia 2000;2:306–14.
[37] Grant DS, Williams TL, Zahaczewsky M, Dicker AP. Comparison of antiangiogenic activities using paclitaxel (taxol) and docetaxel (taxotere). Int J Cancer 2003;104:121–9.
[38] Clements MK, Jones CB, Cumming M, Daoud SS. Antiangiogenic potential of camptothecin and topotecan. Cancer Chemother Pharmacol 1999;44:411–6.
[39] Schirner M. Antiangiogenic chemotherapeutic agents. Cancer Metast Rev 2000;19:67–73.
[40] Kerbel R, Folkman J. Clinical translation of angiogenesis inhibitors. Nat Rev Cancer 2002;2:727–39.